

High energy neutrino emission from the core of low luminosity AGNs triggered by magnetic reconnection acceleration

B. Khiali^{1*} and E. M. de Gouveia Dal Pino¹

¹*IAG-Universidade de São Paulo, Rua do Matão 1226, São Paulo, SP, Brazil*

Accepted 2015 October 6. Received 2015 September 21; in original form 2015 June 02

ABSTRACT

The detection of astrophysical very high energy (VHE) neutrinos in the range of TeV-PeV energies by the IceCube observatory has opened a new season in high energy astrophysics. Energies \sim PeV imply that the neutrinos are originated from sources where cosmic rays (CRs) can be accelerated up to $\sim 10^{17}$ eV. Recently, we have shown that the observed TeV gamma-rays from radio-galaxies may have a hadronic origin in their nuclear region and in such a case this could lead to neutrino production. In this paper we show that relativistic protons accelerated by magnetic reconnection in the core region of these sources may produce HE neutrinos via the decay of charged pions produced by photo-meson process. We have also calculated the diffuse flux of HE neutrinos and found that it can be associated to the IceCube data.

Key words: Low luminosity AGNs- very high energy neutrinos- cosmic ray acceleration: magnetic reconnection- radiation mechanisms: non-thermal.

1 INTRODUCTION

Neutrino observations can provide unique information to understand their origin and can even lead to the discovery of new classes of astrophysical sources. The inherent isotropic nature of the detected neutrino flux by IceCube is compatible with an extragalactic origin and is supported by diffuse high energy γ -ray data (Ahlers & Murase 2014). The observed neutrinos with energies \sim PeV suggest that they are originated from a source where cosmic rays (CRs) can be accelerated up to $\sim 10^{17}$ eV.

A potential mechanism to produce VHE neutrinos in the TeV-PeV range is through the decay of charged pions created in proton-proton (pp) or proton-photon ($p\gamma$) collisions in a variety of astrophysical sources which, in the framework of the IceCube observations, may include active galactic nuclei (AGNs) (Kasanas & Ellison 1986; Stecker et al. 1991; Atoyan & Dermer 2001; Neronov & Semikoz 2002) and gamma-ray bursts (GRBs) (Waxman & Bahcall 1997).

Hadronic mechanisms producing VHE neutrinos via the acceleration of cosmic rays (CRs) in AGNs have been suggested for more than three decades (Eichler 1979; Protheroe & Kasanas 1983; Mannheim 1995; Hazlen & Zas 1997; Mucke & Protheroe 2001; Kalashev et al. 2014; Marinelli & Fraija 2014b; Atoyan & Dermer 2003; Becker 2008). Cur-

rently, the detection of gamma-ray emission at TeV energies in AGNs, not only in high luminous blazars, but also in less luminous radio-galaxies, has strengthened the notion that they may be excellent cosmic ray accelerators and therefore, important potential neutrino emission candidates.

Several recent models have tried to describe the detected TeV neutrino emission as due to AGNs. For instance, Marinelli & Fraija (2014b) employed two different hadronic scenarios involving the interaction of accelerated protons at the AGN jet either with photons produced via synchrotron self-Compton (SSC) or with thermal particles in the giant lobes. They then derived the expected neutrino flux for low luminous AGNs (LLAGNs)¹, or more specifically, for radio galaxies for which they examined the origin of the observed TeV gamma-ray spectra as due to hadronic processes.

Earlier work by Gupta (2008) had already introduced hadronic scenarios to explain the TeV emission in LLAGNs (e.g., Cen A). Also, Fraija (2014a,b) suggested neutral pion decays from pp and $p\gamma$ interactions in these sources as probable candidates to explain the high energy neutrinos. In another model, Kalashev et al. (2014) attempt to reproduce the

¹ By LLAGNs we mean non-blazar sources with $L_{H\alpha} \leq 10^{40}$ ergs⁻¹ (see Ho et al. 1997; Nagar et al. 2005), where $L_{H\alpha}$ is the $H\alpha$ luminosity. These typically consist of liners and seyfert galaxies which are also FR I or FR II radio sources. For more details see Kadowaki et al. (2015).

* E-mail: bkhiali@usp.br

IceCube data using the $p\gamma$ mechanism considering the radiation field produced by the accretion disk around the AGN central black hole (assuming a standard Shakura-Sunyaev accretion disk model). Alternatively, Kimura et al. (2014) calculated the neutrino spectra using the radiatively inefficient accretion flows (RIAF) model in the nuclei of LLAGNs considering both pp and $p\gamma$ mechanisms and stochastic proton acceleration in the RIAF turbulence.

The possibility of producing VHE neutrino emission has been also extensively explored in blazars - AGNs for which the relativistic jet points to the line of sight (e.g., Atoyan & Dermer 2003; Becker 2008; Murase et al. 2014; Dermer et al. 2014). Dermer et al. (2014), in particular, revisited the previous studies assuming that the observed neutrinos could be produced in the inner jet of blazars and concluded that neither the flux nor the spectral shape suggested by the IceCube data could be reproduced by this scenario which predicts a rapid decline of the emission below 1 PeV. Tavecchio et al. 2014 and Tavecchio & Ghisellini 2014, on the other hand, considered the distribution of lower-power blazars, namely, BL Lac objects and, by employing a two-zone spine-sheath jet model to these sources concluded that they might be suitable for the production of the observed PeV neutrinos revealed by the IceCube.

Presently, it is very hard to define what should be the dominant process or the real sources that are producing the observed neutrino flux mainly due to the lack of more precise measurements. But while waiting for better measurements, we can explore further mechanisms and try to make reliable predictions in order to constrain the candidates.

The big challenge in models that rely on hadronic processes in the AGN nuclei is how to produce the relativistic protons that may lead to γ -ray emission and the accompanying neutrino flux. Diffusive shock acceleration at the jet launching base was discussed by Begelman et al. (1990). Levinson (2000) and more recently, Vincent (2014) proposed that TeV gamma-ray emission might be produced in the BH magnetosphere by pulsar-like mechanisms, i.e., with particles being accelerated by the electric potential difference settled by non uniform magnetic field. As remarked above, Kimura et al. (2014) discussed stochastic acceleration in an accreting RIAF turbulent scenario, but currently none of these models can be regarded as dominant or disclaimed given the uncertainties from the observations regarding the location of the gamma-ray emission (see §. 5).

In this work, we consider an alternative acceleration model that may occur in the vicinity of BHs which was explored first in the framework of microquasars by de Gouveia Dal Pino & Lazarian 2005 (hereafter GL05) and then extended to AGNs by de Gouveia Dal Pino, Piovezan & Kadowaki 2010 (hereafter GPK10). In this model, particles can be accelerated in the surrounds of the BH by the magnetic power extracted from events of fast magnetic reconnection occurring between the magnetosphere of the BH and the lines rising from the inner accretion disk into the corona (Figure 1).

More recently, Kadowaki, de Gouveia Dal Pino & Singh (2015) revisited this model exploring different mechanisms of fast magnetic reconnection and extending the study to include also the gamma-ray emission of a large sample of sources (more than 200 sources involving blazars, non-blazars or LLAGNs, and galactic black hole binaries). They

confirmed the earlier trend found by GL05 and GPK10, verifying that the fast magnetic reconnection power calculated as a function of the black hole (BH) mass can explain the observed radio and gamma-ray luminosity from nuclear outbursts of all LLAGNs and galactic black hole binaries of their sample, spanning 10^{10} orders of magnitude in mass (see Fig. 5 in Kadowaki et al. 2015).²

In the works above, a standard accretion disk model was employed, but in an accompanying work (Singh et al. 2015), the authors adopted a magnetically dominated advective flow (MDAF) for the accretion and obtained very similar results to those above, which demonstrated that the details of the accretion physics are not relevant in the development of the magnetic reconnection process and the particle acceleration occurring in the corona.

The magnetic reconnection acceleration model above (see Kadowaki et al. 2015) has been also employed to reproduce the observed multi-wavelength spectral energy distribution (SED) of a few microquasars (Cygnus X-1 and Cygnus X-3) (Khiali, de Gouveia Dal Pino & del Valle (2015), henceforth KGV15) and LLAGNs (Cen A, NGC 1275, M87 and IC310) (Khiali, de Gouveia Dal Pino & Sol (2015), hereafter KGS15), and the results indicate that hadronic mechanisms (pp and $p\gamma$) are the main radiative processes producing the observed GeV to TeV γ -rays.

The results of the works above and in particular, the reproduction of the observed SEDs and the TeV gamma-ray emission of the radio-galaxies by hadronic processes involving particles accelerated by magnetic reconnection in the surrounds of the BH (KGS15), have motivated the present study. We aim here to calculate the spectrum of neutrinos arising from the interactions of accelerated protons by the mechanism above with the radiation and thermal-particle fields around the BH. According to our previous results (KGV15 and KGS15), these interactions produce weakly decaying π^0 and π^\pm pions. The latter may generate high energy neutrinos. We will then evaluate the diffuse neutrino intensity and compare with the IceCube data in the context of LLAGNs.

For completeness, we will also compare the particle acceleration by magnetic reconnection with shock acceleration in the surrounds of the BH.

The outline of the paper is as follows. In Section 2, we describe in detail our scenario. In Section 3, we describe the hadronic interactions and calculate the acceleration and radiative cooling rates. The calculation of the spectrum of neutrinos and their diffuse intensity for comparison with the IceCube data is presented in Section 4. We discuss and summarize our results and conclusions in Section 5.

² We note that the calculated reconnection power in this core model though large enough to explain the luminosity of galactic black hole binaries and LLAGNs (or non-blazars), is insufficient for reproducing the luminosity of most of the blazars and GRBs, which is compatible with the notion that the observed emission in these cases is produced outside the core, at the jet that points to the line of sight and screens any deep nuclear emission (Kadowaki et al. 2015).

2 DESCRIPTION OF THE MODEL

In this section we summarize the main characteristics of our fast magnetic reconnection model in the surrounds of the BH and how particles can be accelerated in the magnetic reconnection layer. For a more detailed description we refer to Kadowaki et al. 2015.

2.1 Fast magnetic reconnection in the surrounds of the BH

We assume that the gamma-ray emission from low-luminous AGNs is produced in the core region and the particles responsible for this emission are accelerated in the corona around the BH and accretion disk as sketched in Figure 1.

Turbulent dynamo inside the accretion disk or plasma dragging from the surrounds can build the large-scale poloidal magnetic fields that arise into the corona. This poloidal magnetic flux under the action of disk differential rotation gives rise to a wind that partially removes angular momentum from the system increasing the accretion rate and the ram pressure of the accreting material that will then press the magnetic lines in the inner disk region against the lines anchored into the BH horizon allowing them to reconnect (see Fig. 1). The magnetic field intensity in the inner region of the accretion disk corona is approximately given by the balance between the magnetic pressure of the BH magnetosphere and the accretion ram pressure (Kadowaki et al. 2015):

$$B \cong 9.96 \times 10^8 r_X^{-1.25} \xi^{0.5} m^{-0.5} \text{ G}. \quad (1)$$

Where $r_X = R_X/R_S$ is the inner radius of the accretion disk in units of the BH Schwartzchild radius (R_S) (in our calculations we assume $r_X = 6$); ξ is the mass accretion disk rate in units of the Eddington rate ($\xi = \dot{M}/\dot{M}_{Edd}$), with $\dot{M}_{Edd} = 1.45 \times 10^{18} m \text{ g s}^{-1}$), which we assume to be $\xi \simeq 0.7^3$; m is the BH mass in units of solar mass.

The presence of embedded turbulence in the nearly collisional MHD coronal flow of the core region of the AGNs can make reconnection very fast with a rate $V_R \simeq v_A (l_{inj}/L)^{1/2} (v_{turb}/v_A)^2$, where l_{inj} and v_{turb} are the injection scale and velocity of the turbulence, respectively (e.g., Lazarian & Vishniac 1999, hereafter LV99⁴). This relation shows that the reconnection rate is of the order of the Alfvén speed v_A , which in the systems here considered may be near the light speed.

The magnetic reconnection power released by turbulent driven fast reconnection in the magnetic discontinuity region (Figure 1) is given by (Kadowaki et al. 2015):

$$W \simeq 1.66 \times 10^{35} \psi^{-0.5} r_X^{-0.62} l^{-0.25} l_X q^{-2} \xi^{0.75} m \text{ erg s}^{-1}, \quad (2)$$

³ See Fig. 5 in Kadowaki et al. (2015). Accretion rates ξ between $0.05 < \xi \leq 1$ are able to produce magnetic reconnection power values which are enough to probe the observed gamma-ray luminosities from LLAGNs.

⁴ According to the LV99 model, even weak embedded turbulence causes the wandering of the magnetic field lines which allows for many independent patches to reconnect simultaneously making the global reconnection rate large (for more details see Kadowaki et al. 2015). This theory has been confirmed numerically by means of 3D MHD simulations (Kowal et al. 2009, 2012).

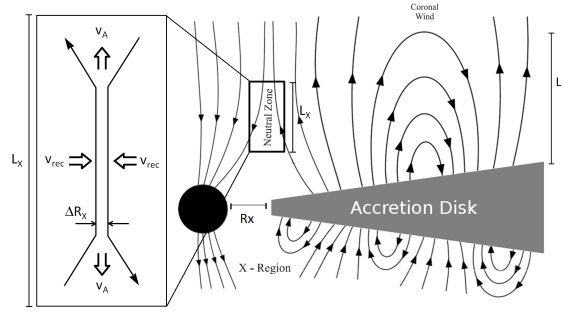


Figure 1. Scheme of magnetic reconnection between the lines arising from the accretion disk and the lines anchored into the BH horizon. Reconnection is made fast by the presence of embedded turbulence in the reconnection (neutral) zone (see text for more details). Particle acceleration may occur in the magnetic reconnection zone by a first-order Fermi process (adapted from GL05).

where $l = L/R_S$ is the height of the corona in units of R_S ; $l_X = L_X/R_S$, L_X is the extension of the magnetic reconnection zone (as shown in Figure 1), $q = [1 - (3/r_X)^{0.5}]^{0.25}$ and $v_A = v_{A0}\psi$ is the relativistic form of the Alfvén velocity, with $v_{A0} = B/(4\pi\rho)^{1/2}$, B being the local magnetic field, $\rho \simeq n_c m_p$ the fluid density, and $\psi = [1 + (v_{A0}/c)^2]^{-1/2}$, in this work, we find that $v_{A0} \sim c$.

The acceleration region in our model corresponds to the cylindrical shell around the BH where magnetic reconnection takes place, as shown in Figure 1. This shell has a length l_X , with inner and outer radii given by R_X and $R_X + \Delta R_X$ respectively, where ΔR_X is the width of the current sheet given by (Kadowaki et al. 2015):

$$\Delta R_X \cong 2.34 \times 10^4 \psi^{-0.31} r_X^{0.48} l^{-0.15} l_X q^{-0.75} \xi^{-0.15} m \text{ cm}. \quad (3)$$

This magnetic reconnection power (Eq. 2) will both heat the surrounding gas and accelerate particles. As in Kadowaki et al. (2015), we assume that approximately 50% of the reconnection power goes to accelerate the particles (see §. 2.2.). This is consistent with plasma laboratory experiments of reconnection acceleration (Yamada et al. 2014) and also with the observations of solar flares (e.g., Lin & Hudson 1971). We further assume that this power is equally shared between the protons and electrons/positrons, so that the proton luminosity will be 25% of the calculated value by Eq. 2.

The particle density in the coronal region in the surrounds of the BH is (Kadowaki et al. 2015):

$$n_c \cong 8.02 \times 10^{18} r_X^{-0.375} \psi^{0.5} l^{-0.75} q^{-2} \xi^{0.25} m^{-1} \text{ cm}^{-3}. \quad (4)$$

2.2 Particle acceleration due to the magnetic power released by fast reconnection

In the magnetic reconnection layer (or current sheet; see Figure 1) where the two converging magnetic flux tubes move to each other with a velocity V_R , trapped particles may bounce back and forth due to head-on collisions with magnetic fluctuations in the current sheet. As a consequence, their energy after a round trip may increase by $\langle \Delta E/E \rangle \sim V_R/c$, implying an exponential energy increase after several round trips. This first-order Fermi acceleration process within re-

connection layers was first studied by GL05 and successfully tested through 3D MHD simulations with test particles injected in current sheets with fast reconnection driven by turbulence (Kowal et al. 2011, 2012; see also (de Gouveia Dal Pino, Kowal & Lazarian 2014; de Gouveia Dal Pino & Kowal 2015 for reviews)⁵.

From the results of the 3D MHD numerical simulations (Kowal et al. 2012), we find that the acceleration rate for a proton is given by (see also KGV15):

$$t_{acc,M.R.,p}^{-1} = 1.3 \times 10^5 \left(\frac{E}{E_0} \right)^{-0.4} t_0^{-1}, \quad (5)$$

where E is the energy of the accelerated proton, $E_0 = m_p c^2$, m_p is the proton rest mass, $t_0 = l_{acc}/v_A$ is the Alfvén time, and l_{acc} is the length scale of the acceleration region and for electrons this rate is (KGV15):

$$t_{acc,M.R.,e}^{-1} = 1.3 \times 10^5 \sqrt{\frac{m_p}{m_e}} \left(\frac{E}{E_0} \right)^{-0.4} t_0^{-1}, \quad (6)$$

where m_e is the electron rest mass.

As stressed in GL05 (see also KGV15 and KGS15), it is also possible that a diffusive shock may develop in the surrounds of the magnetic reconnection zone due to coronal mass ejections released by fast reconnection along the magnetic field lines, as observed in solar flares. A similar picture has been also suggested by e.g., Romero et al. (2010b). In this case, the shock velocity will be predominantly parallel to the magnetic field lines and the acceleration rate for a particle of energy E in a magnetic field B , will be approximately given by (e.g., Spruit 1988):

$$t_{acc,shock}^{-1} = \frac{\eta e c B}{E}, \quad (7)$$

where $0 < \eta \ll 1$ characterizes the efficiency of the acceleration. We fix $\eta = 10^{-2}$, which is appropriate for shocks with velocity $v_s \approx 0.1c$, which are commonly assumed in the Bohm regime (Romero et al. 2010b).

3 HADRONIC INTERACTIONS

In KGS15, we have demonstrated that the core region of LLAGNs is able to accelerate protons up to energies of a few 10^{17} eV through the first-order Fermi magnetic reconnection mechanism described in the previous section. This indicates that these sources could be powerful CR accelerators. We show below that these protons can cool very efficiently via synchrotron, $p\gamma$ and pp interactions in the region that surrounds the BH of these sources (Figure 2). As remarked, these hadronic interactions lead to the production of HE γ -rays and HE neutrinos via decays of neutral and charged pions, respectively. In KGS15, we have calculated the spectral energy distribution of the HE γ -ray emission for the LLAGNs for which this emission has been detected. Below, we calculate the HE neutrino emission from the nuclear region of these sources.

⁵ Particle acceleration within reconnection sheets has been also extensively tested numerically in collisionless fluids by means of 2D (e.g., Zenitani & Hoshino 2001; Drake et al. 2006, 2010; Cerutti et al. 2013) and 3D particle in cell simulations (Sironi & Spitkovsky 2014).

Table 1. Three sets of model parameters for LLAGNs.

Parameters	Model 1	Model 2	Model 3
m BH mass (M_\odot)	10^7	10^8	10^9
p Injection spectral index	1.9	1.7	2.2

3.1 pp collisions

The charged pions can be created through inelastic collisions of the relativistic protons with nuclei of the corona that surrounds the BH and the accretion disk by means of the following reactions (Atoyan & Dermer 2003; Becker 2008)

$$p + p \rightarrow n_1(\pi^+ + \pi^-) + n_2\pi^0 + p + p \quad (8)$$

where n_1 and n_2 are multiplicities, $\pi^0 \rightarrow \gamma + \gamma$ (Stecker 1970, 1971), carrying 33% of the accelerated proton's energy. The charged pions π^\pm then decay and produce neutrinos via $\pi^+ \rightarrow \nu_\mu + \bar{\nu}_\mu + \nu_e + e^+$ and $\pi^- \rightarrow \nu_\mu + \bar{\nu}_\mu + \bar{\nu}_e + e^-$, where ν_μ , $\bar{\nu}_\mu$, and ν_e are the muon neutrino, muon antineutrino, and electron neutrino, respectively (Margolis et al. 1978; Stecker 1979; Michalak et al. 1990). The pp cooling rate is almost independent of the proton energy and is given by (Kelner 2006)

$$t_{pp}^{-1} = n_i c \sigma_{pp} k_{pp}, \quad (9)$$

where, n_i is the coronal number density of protons which can be calculated by eq. 4, and k_{pp} is the total inelasticity of the process of value ~ 0.5 . The corresponding cross section for inelastic pp interactions σ_{pp} can be approximately by (Kelner et al. 2009)

$$\sigma_{pp}(E_p) = (34.3 + 1.88Q + 0.25Q^2) \left[1 - \left(\frac{E_{th}}{E_p} \right)^4 \right]^2 \text{ mb}, \quad (10)$$

where mb stands for milli-barn, $Q = \ln \left(\frac{E_p}{1 \text{ TeV}} \right)$, and the proton threshold kinetic energy for neutral pion (π^0) production is $E_{th} = 2m_\pi c^2 (1 + \frac{m_\pi}{4m_p}) \approx 280$ MeV, where $m_\pi c^2 = 134.97$ MeV is the rest energy of π^0 (Villa & Aharonian 2009). This particle decays in two photons with a probability of 98.8%.

3.2 $p\gamma$ interactions

The photomeson ($p\gamma$) production takes place for photon energies greater than $E_{th} \approx 145$ MeV. Pions are also obtained from the $p\gamma$ interaction near the threshold via the channels (Atoyan & Dermer 2003)

$$p + \gamma \rightarrow p + \pi^0, \quad (11)$$

with $\pi^0 \rightarrow \gamma + \gamma$ carrying 20% of accelerated protons energy and

$$p + \gamma \rightarrow p + \pi^+ + \pi^-, \quad (12)$$

and the charged pions will also decay producing neutrinos as described in §. 3.1.

The radiative cooling rate for this mechanism in an isotropic photon field with density $n_{ph}(E_{ph})$ can be calculated by (Stecker 1968):

$$t_{p\gamma}^{-1}(E_p) = \frac{c}{2\gamma_p^2} \int_{\frac{E_{th}(\pi)}{2\gamma_p}}^{\infty} dE_{ph} \frac{n_{ph}(E_{ph})}{E_{ph}^2} \times \int_{\frac{E_{th}(\pi)}{2\gamma_p}}^{2E_{ph}\gamma_p} d\epsilon_r \sigma_{p\gamma}^{(\pi)}(\epsilon_r) K_{p\gamma}^{(\pi)}(\epsilon_r) \epsilon_r, \quad (13)$$

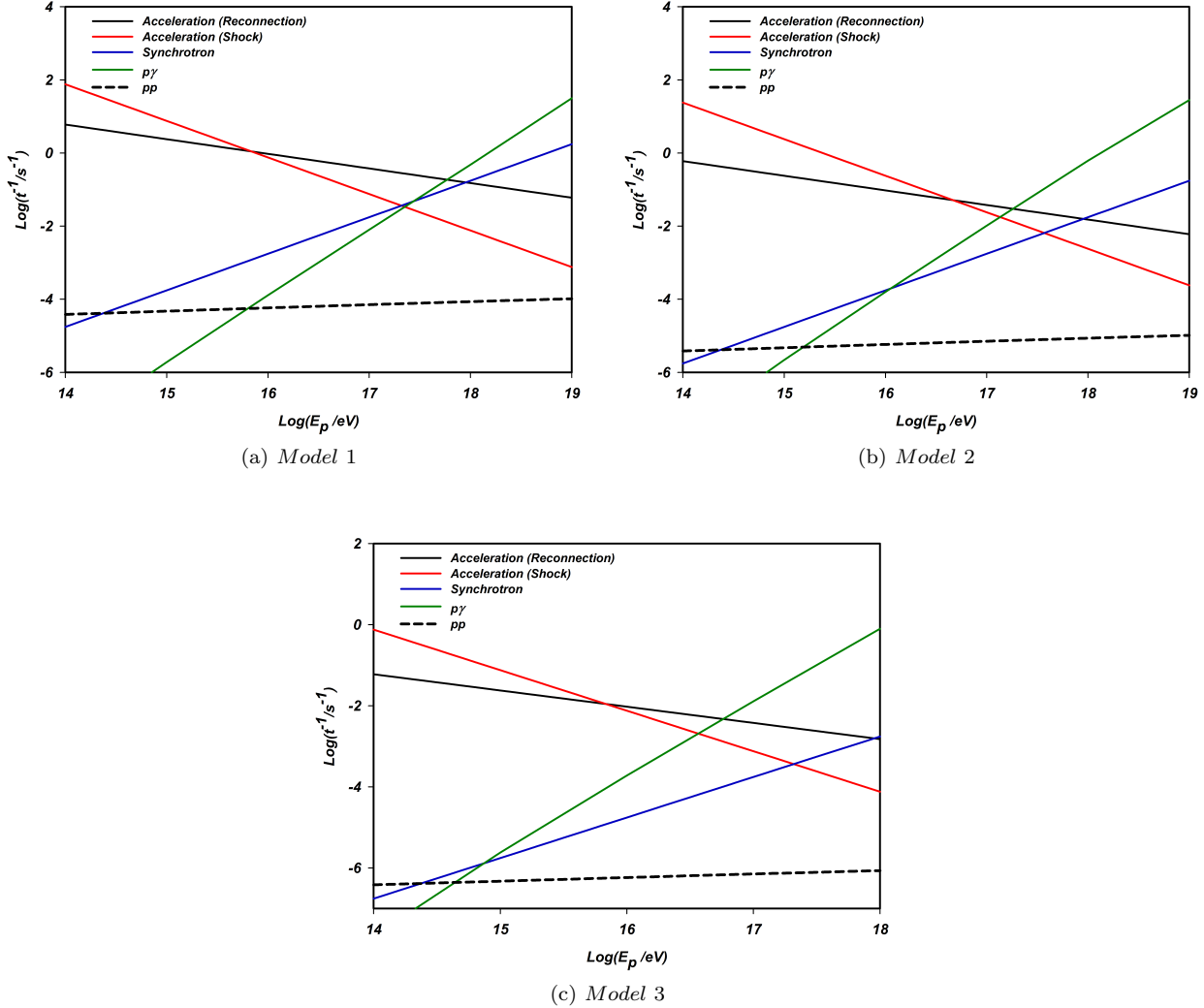


Figure 2. Acceleration and cooling rates for protons in the core regions of LLAGNs with a central black hole mass (a) $M = 10^7 M_\odot$ (Model 1), (b) $M = 10^8 M_\odot$ (Model 2), and (c) $M = 10^9 M_\odot$ (Model 3).

where in our model the appropriate photons come from the synchrotron radiation⁶, $n_{ph}(E_{ph}) = n_{synch}(\epsilon)$, $\gamma_p = \frac{E_p}{m_e c^2}$, ϵ_r is the photon energy in the rest frame of the proton, and $K_{p\gamma}^{(\pi)}$ is the inelasticity of the interaction. Atoyan & Dermer (2003) proposed a simplified approach to calculate the cross-section and the inelasticity which are given by

$$\sigma_{p\gamma}(\epsilon_r) \approx \begin{cases} 340 \mu\text{barn} & 300\text{MeV} \leq \epsilon_r \leq 500\text{MeV} \\ 120 \mu\text{barn} & \epsilon_r > 500\text{MeV}, \end{cases} \quad (14)$$

and

$$K_{p\gamma}(\epsilon_r) \approx \begin{cases} 0.2 & 300\text{MeV} \leq \epsilon_r \leq 500\text{MeV} \\ 0.6 & \epsilon_r > 500\text{MeV}. \end{cases} \quad (15)$$

⁶ We find that for photomeson production, the radiation from the accretion disk is irrelevant compared to the contribution from the coronal synchrotron emission above the disk (see KGV15 and KGS15 for a detailed derivation of the synchrotron rate and its radiation field density).

4 NEUTRINO EMISSION AND DIFFUSE INTENSITY

To calculate the neutrino emission from the nuclear region of an LLAGN, we consider a population of protons accelerated by magnetic reconnection in the surrounds of the BH according to the model described in Section 2.

We assume for these accelerated particles an isotropic power law spectrum (in units of $\text{erg}^{-1}\text{cm}^{-3}\text{s}^{-1}$) (see e.g. KGV15 and references there in):

$$Q(E) = Q_0 E^{-p} \exp[-E/E_{max}] \quad (16)$$

where $p > 0$ and E_{max} is the cut-off energy.

The normalization constant Q_0 above is calculated from the total power injected to accelerate the protons according to the relation:

$$L_p = \int_V d^3r \int_{E_{min}}^{E_{max}} dE E Q(E) \quad (17)$$

where V is the volume of the emission region around the

magnetic reconnection zone and L_p corresponds to the magnetic reconnection power W given by Eq. 2. To calculate W we have adopted the following suitable set of parameters $\xi = 0.7$, $R_X = 6R_S$, $L_X = 10R_S$, and $L = 20R_S$.

The maximum energy of the accelerated particles E_{max} is derived from the balance between the magnetic reconnection acceleration rate (Eq. 5) and the radiative loss rates as given in Section 3. Figure 2 compares these rates for protons considering LLAGNs with three different BH masses 10^7 , 10^8 and $10^9 M_\odot$. We have also considered different power-law indices (p) for the injected particle spectrum in each of these models (see Table 1) which are compatible with the values derived from analytical and numerical studies of first-order Fermi acceleration by magnetic reconnection and also with values inferred from the observations (e.g., KGS15). The calculated values of B , W , ΔR_X and n_c from Eqs. 1-4 for these three representative source models are listed in Table 2. For simplicity, we consider the derived proton luminosities (which are $\sim 1/4W$) and the emission properties of these three models to characterize the whole range of LLAGNs in the calculation of the HE neutrino flux below. The adoption of this approach, rather than accounting for a whole range of BH mass sources allows us to avoid the introduction of further free parameters in the modelling.

In Fig. 2, for comparison we have also calculated the proton acceleration rate due to a shock formed in the surrounds of the reconnection region (Eq. 7) for the same set of parameters as above. As in KGV15 and KGS15, we find that the maximum energy attained from magnetic reconnection acceleration is higher than that from the shock. It should be also remarked that protons with these calculated maximum energies have Larmor radii smaller than the thickness of the reconnection layer ΔR_X (eq. 3), as required.

The neutrinos that are produced from pion decay will escape from the emission region without any absorption and their spectrum is given by (Tavecchio et al. 2014; Kimura et al. 2014):

$$E_\nu L_\nu(E_\nu) \simeq (0.5t_{pp}^{-1} + \frac{3}{8}t_{p\gamma}^{-1}) \frac{L_X}{c} E_p L_p, \quad (18)$$

where E_ν is the neutrino energy and E_p the proton energy. Since Figure 2 demonstrates that the $p\gamma$ emission cools the protons faster than pp collisions, the dominant hadronic process in our model is the $p\gamma$ emission. Therefore, this mechanism will prevail in the production of the neutrinos and the first term of eq. 18 can be neglected. In $p\gamma$ interactions, E_ν is related with the parent proton energy through the equation $E_\nu = 0.05E_p$ (Spurio 2015), because the average energy of the pion is ~ 0.2 of the parent proton energy and in the decay of the π^+ chain four leptons are produced (including one electron neutrino as remarked), each of which has roughly 1/4 of the pion energy. It has been also demonstrated in Spurio (2015) that the ratio of the neutrino luminosity to the photon luminosity from $p\gamma$ interactions is $\sim 1/3$.

In consistency with the statement above, the maximum energy of the produced neutrinos can be calculated from $E_{\nu,max} = 0.05E_{p,max}$ (Becker 2008; Hazlen 2007), which according to our model is $\sim 3 \times 10^{16}$ eV for a source with a black hole mass $M_{BH} = 10^7 M_\odot$, $\sim 5 \times 10^{15}$ eV for a source with $M_{BH} = 10^8 M_\odot$, and $\sim 2 \times 10^{15}$ eV for a source with $M_{BH} = 10^9 M_\odot$.

The total diffuse neutrino intensity from the extragalac-

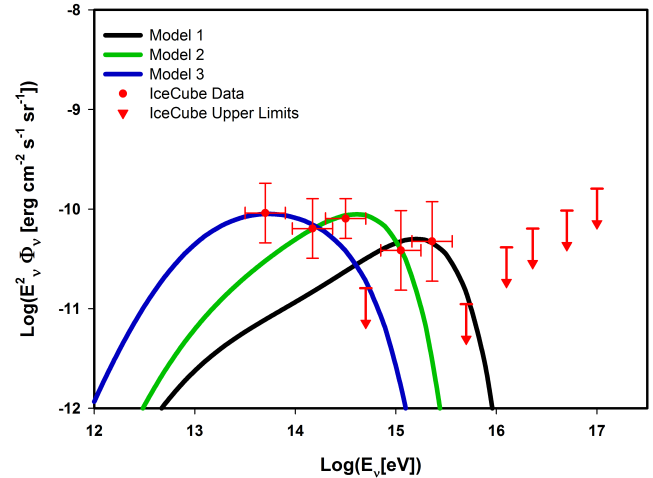


Figure 3. Calculated diffuse intensity of neutrinos from the cores of LLAGNs considering our magnetic reconnection acceleration model to produce the protons and gamma-ray photons for three different BH masses. The data are taken from IceCube measurements (Aartsen et al. 2014).

tic sources we are considering here, i.e., LLAGNs may have contributions from different redshifts. Neglecting evolutionary effects in the core region of these sources, we can estimate the total intensity as (Murase et al. 2014)

$$\Phi_\nu = \frac{c}{4\pi H_0} \int_0^{z_{max}} dz \frac{1}{\sqrt{(1+z)^3 \Omega_m + \Omega_\Lambda}} \times \int_{L_{min}}^{L_{max}} dL_\gamma \rho_\gamma(L_\gamma, z) \frac{L_\nu(E_\nu)}{E_\nu}, \quad (19)$$

where L_γ is the γ -ray luminosity, and $\rho_\gamma(L_\gamma, z)$ is the γ -ray luminosity function (GLF) of the core of the sources, defined as the number density of sources per unit comoving volume, per unit logarithmic luminosity between the redshifts $z = 0$ to $z = z_{max}$, being the latter the maximum observed redshift for radiogalaxies, $z_{max} \simeq 5.2$ (Klamer et al. 2005). GLF is integrated from L_{min} to L_{max} which are obtained from *Fermi*-LAT observations and are given by 10^{41} and 10^{44} erg/s, respectively (Di Mauro et al. 2014). The values for the cosmological parameters are assumed as: $H_0 = 70$ km s $^{-1}$ Mpc $^{-1}$, $\Omega_M = 0.3$ and $\Omega_\Lambda = 0.7$.

We evaluate the GLF, $\rho_\gamma(L_\gamma, z)$ as in Di Mauro et al. (2014), from the estimated radio luminosity function (RLF) which for non-blazars is given by

$$\rho_\gamma(L_\gamma, z) = \rho_{r,tot}(L_{r,tot}^{5\text{GHz}}(L_{r,core}^{5\text{GHz}}(L_\gamma)), z) \times \frac{d \log L_{r,core}^{5\text{GHz}}}{d \log L_\gamma} \frac{d \log L_{r,tot}^{5\text{GHz}}}{d \log L_{r,core}^{5\text{GHz}}}. \quad (20)$$

$d \log L_{r,core}^{5\text{GHz}}/d \log L_\gamma$ and $d \log L_{r,tot}^{5\text{GHz}}/d \log L_{r,core}^{5\text{GHz}}$ can be calculated by (Di Mauro et al. 2014)

$$\log L_\gamma = 2.00 \pm 0.98 + (1.008 \pm 0.025) \log(L_{r,core}^{5\text{GHz}}), \quad (21)$$

and

$$\log L_{r,core}^{5\text{GHz}} = 4.2 \pm 2.1 + (0.77 \pm 0.08) \log(L_{r,tot}^{5\text{GHz}}), \quad (22)$$

where $L_{r,tot}^{5\text{GHz}}$ and $L_{r,core}^{5\text{GHz}}$ are the radio total and

Table 2. Physical conditions around the LLAGNs represented by models 1, 2 and 3, obtained from Eqs. 1 to 4, using $r_x = 6$, $l = 20$, $l_X = 10$ and $\xi = 0.7$.

	Parameters	Model 1	Model 2	Model 3
B	Magnetic field (G)	2.8×10^4	8874	2806
W	Magnetic reconnection power (erg/s)	2.4×10^{42}	2.4×10^{43}	2.4×10^{44}
ΔR_X	Width of the current sheet (cm)	7.2×10^{12}	7.2×10^{13}	7.2×10^{14}
n_c	Coronal particle number density (cm^{-3})	3.6×10^{10}	3.6×10^9	3.6×10^8

core luminosities, respectively. The total RLF, $\rho_{r,tot}(L_{r,tot}(L_{r,core}^{5\text{GHz}}(L_\gamma)), z)$, is found from interpolation of the observed data for radio-galaxies provided by Yuan & Wang (2012):

$$\begin{aligned} \rho_{r,tot}(L_{r,core}^{5\text{GHz}}(L_\gamma), z) = & (-1.1526 \pm 0.0411) \log L_{r,core}^{5\text{GHz}} \\ & + (0.5947 \pm 0.1224)z + 23.2943 \\ & \pm 1.0558 \text{ Mpc}^{-3} (\log L_{r,core}^{5\text{GHz}})^{-1}. \end{aligned} \quad (23)$$

The resulting neutrino flux is shown in Figure 3. It was calculated using eq. 19 above, considering the maximum neutrino energies obtained for sources with the three different BH masses (as in Figure 2).

Sources with $M_{BH} = 10^7 M_\odot$ result a spectrum that matches better with the observed most energetic part of the neutrino flux by the IceCube, at $\sim 3 \times 10^{15}$ to 10^{16} eV, while sources with BH masses of the order of $10^8 M_\odot$ produce a spectrum that nearly fits the observed neutrinos flux in the range of $10^{14} - 10^{15}$ eV, and sources with mass $\sim 10^9 M_\odot$ the narrow energy band 5×10^{13} eV – 10^{14} eV as well as the upper limit at 5×10^{14} eV.

5 DISCUSSION AND CONCLUSIONS

In this work we have explored a model to describe the observed flux of extragalactic very high energy (VHE) neutrinos by the IceCube (Aartsen et al. 2014) in the framework of low luminosity AGNs (LLAGNs), or more specifically, of radio-galaxies. The recent detection of gamma-ray emission in the TeV range in these sources makes them also potential candidates of VHE neutrino emission via the decay of charged pions which can be produced by the interaction of accelerated relativistic protons with ambient lower energy photons and protons.

We have examined here a fast magnetic reconnection mechanism in the surrounds of the central BH occurring between the lines lifting from the accretion disk into the corona and those of the BH magnetosphere to accelerate particles to relativistic energies through a first-order Fermi process in the reconnection layer (GL05, Kowal et al. 2012). Recently, it has been demonstrated that this model successfully reproduces the observed gamma-ray luminosity of hundreds of LLAGNs (Kadowaki et al. 2015 and SGK15) and also shapes the SEDs of several radio-galaxies, particularly reproducing their TeV gamma-ray energies mainly via photomeson ($p\gamma$) interactions (KGS15).

Applying the same acceleration model as above (see Section 2), considering three different BH masses, we have shown that also the observed VHE neutrino Icecube flux (Aartsen et al. 2014) can be obtained from the decay of

charged pions produced in photomeson interactions involving the accelerated protons and Synchrotron photons in the core region of these sources (Figs. 2 and 3).

Specifically, in Fig. 2, we compared the magnetic reconnection acceleration rate (derived from the numerical simulations of Kowal et al. (2012) and calculated for the source parameters) with the relevant hadronic cooling processes and obtained the maximum energy for the accelerated protons mainly constrained by the $p\gamma$ interactions. In Fig. 2, we also compared the magnetic reconnection with the shock acceleration rate in the surrounds of the BH for the same parametric space and demonstrated the higher efficiency of the first process in this region. According to our results in Fig. 2, protons are able to accelerate up to energies of the order of $\sim 10^{17}$ eV and therefore, are suitable to produce 0.1-1 PeV neutrinos.

Fig. 3 indicates that the observed neutrino flux in the few PeV range can be matched by sources with $M_{BH} \sim 10^7 M_\odot$ (Model 1), while the flux in the energy range of $0.1\text{PeV} < E_\nu < 1\text{PeV}$ can be matched by sources with $M_{BH} \sim 10^8 M_\odot$ (model 2), and that in the range $\leq 0.1\text{PeV}$ can be fitted by sources with $M_{BH} \sim 10^9 M_\odot$ (model 3).

We note that, although the calculated neutrino flux was obtained from the integration of the contributions of LLAGNs over the redshifts between $z=0$ and 5.2 (eq. 19) considering, for simplicity, sources with only three characteristic values of BH masses, one may naturally expect that a continuous integration considering the sources with all possible BH masses within the range $10^7 - 10^9 M_\odot$ should provide a similar fitting to the observed data. We also note that our model is unable to explain the IceCube upper limits at the $\sim 10\text{PeV}$ range (also depicted in Fig. 3), which are probably due to other astrophysical compact source population.

Furthermore, we expect that with the 10-fold increased sensitivity at TeV energies, and the larger field of view and improved angular resolution of the forthcoming gamma-ray observatory CTA (Actis et al. 2011; Acharya et al. 2013), the list of LLAGNs with confirmed detection of gamma-ray emission at TeV energies (which currently has only four sources: Cen A, Per A, M87 and IC310), will increase substantially, allowing for a more precise evaluation of the contribution of individual sources for the IceCube neutrino flux.

As remarked in §. 1, other models have been proposed in the literature to explain the IceCube neutrino flux which cannot be discarded or confirmed, considering the current poorness of the data available.

Tavecchio et al. (2014) and Tavecchio & Ghisellini (2014), for instance, have proposed that the lower power blazar class of BL Lac objects could be promising candidates to produce the observed neutrino flux. In their two-zone jet model, the neutrinos are produced by photomeson interactions involving photons emitted in the slower, outer layer that envelopes the faster inner jet component. A lim-

itation of this model is that the high-energy cut-off of the accelerated protons, as well as their injected power are free parameters, unlike in our model where both quantities are directly obtained from the magnetic reconnection acceleration mechanism. Besides, since the BL Lacs are a subclass of the blazars, another difficulty with this model is that it is not clear whether the remaining more powerful blazars, which are also TeV gamma-ray emitters, can or cannot produce neutrinos. According to the recent studies of Dermer et al. (2014) and Murase et al. (2014), which employed a single zone jet model, the powerful blazars would not be suitable candidates to explain the IceCube data. These analyses and the relatively large number of free parameters employed in the evaluation of the neutrino flux leave the question on whether or not blazars do contribute to the IceCube data opened.

Another model to explain the observed neutrino flux has been proposed by Kalashev et al. (2014) who studied photo-pion production on the anisotropic photon field of a Shakura-Sunyaev accretion disk in the vicinity of the BH in AGNs. But this model does not provide an acceleration mechanism either and therefore, the proton high energy cut-off is also a free parameter.

Recently, radio galaxies have been also discussed as possible sources of the observed HE neutrinos by Becker et al. (2014). They demonstrated that FR I radio galaxies would be more probable sources of this emission than FR II radio galaxies. In this work, as we considered the global diffuse contribution from LLAGNs spread over a range of z values, we cannot distinguish the relative contributions from both classes.

Finally, another recent study (Kimura et al. 2014) speculates that the protons responsible for the neutrino emission could be accelerated stochastically by the turbulence induced in a RIAF accretion disk in the core region of LLAGNs. This acceleration process should be essentially a second-order Fermi process and therefore, less efficient than a first-order Fermi process. Nevertheless, their analytically estimated acceleration rate $t_{acc}^{-1} \propto E^{-0.35}$ seems to be too large when compared to that predicted for first-order Fermi processes, as for instance in the present study where the acceleration rate has been extracted directly from 3D MHD simulations with test particles ($t_{acc}^{-1} \propto E^{-0.4}$; Kowal et al. 2012, KGV15), or in shock acceleration (for which analytic predictions give $t_{acc}^{-1} \propto E^{-1}$ (Spruit 1988)). Furthermore, since the candidates to produce PeV neutrinos in this case are radio-galaxies, which are the observed γ -ray emitters, it seems that the employment of the gamma-ray luminosity function (GLF; Di Mauro et al. 2014) to calculate the diffuse neutrino intensity as we did here seems to be more appropriate than the employment of the luminosity function in X-rays, as these authors considered.

In summary, in spite of its simplicity, the numerically tested acceleration model applied to the core region of LLAGNs here presented indicates that LLAGNs are very promising candidates to explain the IceCube VHE neutrinos.

ACKNOWLEDGEMENTS

This work has been partially supported by grants of the Brazilian agencies FAPESP (2013-10559-5, and 2011/53275-4), CNPq (306598/2009-4) and CAPES. We are also indebted to the referee for his/her useful comments.

REFERENCES

- Aartsen, M. G., Ackermann, M., Adams, J., et al. 2014, *Physical Review Letters*, 113, 101101
- Acharya, B. S., Actis, M., Aghajani, T., et al. 2013, *Astroparticle Physics*, 43, 3
- Actis, M., Agnetta, G., Aharonian, F., et al. 2011, *Experimental Astronomy*, 32, 193
- Ahlers, M., & Murase, K. 2014, *Phys. Rev. D*, 90, 023010
- Atoyan, A. M., & Dermer, C. D. 2001, *PRL*, 87, 221102
- Atoyan, A. M., & Dermer, C. D. 2003, *ApJ*, 586, 79
- Becker, J. K. 2008, *Phys. Rep.*, 458, 173
- Becker Tjus, J., Eichmann, B., Halzen, F., Kheirandish, A., & Saba, S. M. 2014, *Phys. Review D*, 89, 123005
- Begelman, M. C., Rudak, B., & Sikora, M. 1990, *ApJ*, 362, 38
- Cerutti, B., Werner, G. R., Uzdensky, D. A., Begelman, M. C. 2013, *ApJ*, 770, 147C
- de Gouveia Dal Pino, E. M. & Lazarian, A. 2005, *Astronomy and Astrophysics*, 441, 845 (GL05)
- de Gouveia Dal Pino, E. M., Piovezan, P. P. & Kadowaki, L. H. S. 2010a, *Astronomy and Astrophysics*, 518, A5
- de Gouveia Dal Pino, E. M., Kowal, G., Lazarian, A. 2014, 8th International Conference of Numerical Modeling of Space Plasma Flows (ASTRONUM 2013), 488, 8, arXiv1401.4941D
- de Gouveia Dal Pino, E. M., & Kowal, G. 2015, in *Magnetic Fields in Diffuse Media* (eds. A. Lazarian, E. M. de Gouveia Dal Pino, C. Melioli), *Astrophysics and Space Science Library*, 407, 373
- Dermer, C. D., Murase, K., & Inoue, Y. 2014, *Journal of High Energy Astrophysics*, 3, 29
- Di Mauro, M., Calore, F., Donato, F., Ajello, M., & Lattorico, L. 2014, *ApJ*, 780, 161
- Drake, J. F., Swisdak, M., Che, H. and Shay, M. A. 2006, *Nature*, 443, 553D
- Drake, J. F., Opher, M., Swisdak, M. and Chamoun, J. N. 2010, *ApJ*, 709, 963D
- Eichler, G. 1979, *ApJ*, 232, 106
- Frajia, N. 2014a, *MNRAS*, 441, 1209
- Frajia, N. 2014b, *ApJ*, 783, 44
- Gupta, N. 2008, *JCAP*, 06, 022
- Hazlen, F. & Zas, E. 1997, *ApJ*, 488, 669
- Hazlen, F. 2007, *ApS&S*, 309, 407
- Ho, L. C., Filippenko, A. V., & Sargent, W. L. W. 1997, *ApJS*, 112, 315
- Kadowaki, L. H. S., de Gouveia Dal Pino, E. M., & Singh, C. B. 2015, *ApJ*, 802, 113
- Kalashev, O., Semikoz, D. & Tkachev, I. 2014, arXiv:1410.8124
- Kazanas, D., & Ellison, D. C. 1986, *ApJ*, 304, 178
- Kelner, S. R., Aharonian, F. A., & Bugayov, V. V. 2006, *Phys.Rev. D*, 74, 0330108
- Kelner, S. R., Aharonian, F. A., & Bugayov, V. V. 2009, *Phys.Rev. D*, 79, 039901

- Khiali, B., de Gouveia Dal Pino, E. M. & del Valle, M. V. 2015a, MNRAS, 449, 34 (KGV15)
- Khiali, B., de Gouveia Dal Pino, E. M. & Sol, H. 2015b, arXiv:1504.07592 (KGS15)
- Kimura, S. S., Murase, K. & Toma, K. 2014, arXiv:1411.3588
- Klamer, I. J., Ekers, R. D., Sadler, E. M., et al. 2005, ApJL, 621, L1
- Kowal, G., Lazarian, A., Vishniac, E. T., Otmianowska-Mazur, K. 2009, ApJ, 700, 63
- Kowal, G., de Gouveia Dal Pino, E. M., Lazarian, A. 2011, The Astrophysical Journal, 735, 102
- Kowal, G., de Gouveia Dal Pino, E. M., Lazarian, A. 2012, Physical Review Letters, 108, 241102
- Lazarian, A., & Vishniac, E. T. 1999, The Astrophysical Journal, 517, 700
- Lazarian, A., & Yan, H. 2014, ApJ, 784, 38
- Levinson, A., 2000, Phys. Rev. Lett., 85, 912
- Lin, R. P., & Hudson, H. S. 1971, SoPh, 17, 412
- Mannheim, K. 1995, APh, 3, 295
- Margolis, S. H., Schramm, D. N., & Silberberg, R. 1978, ApJ, 221, 990
- Marinelli, A., Fraija, N., & Patricelli, B. 2014a, arXiv:1410.8549
- Marinelli, A., & Fraija, N. 2014b, arXiv:1411.2695
- Meier, D. L., 2012, Black Hole Astrophysics: The Engine Paradigm, Springer Verlag, Berlin Heidelberg
- Merloni, A., Heinz, S., & di Matteo, T. 2003, MNRAS, 345, 1057
- Michalak, W., Wdowczyk, J., & Wolfendale, A. W. 1990, Journal of Physics G Nuclear Physics, 16, 1917
- Mucke, A., & Protheroe, J. P. 2001, Astrop. Phys., 15, 121
- Murase, K. 2007, Phys. Rev. D 76, 123001
- Murase, K., Inoue, Y., & Dermer, C. D. 2014, PhRvD, 90, 023007
- Nagar, N. M., Falcke, H., & Wilson, A. S. 2005, A&A, 435, 521
- Neronov, A., & Semikoz, D. V. 2002, Phys. Rev. D 66, 123003
- Protheroe, R. J. & Kasanas, D. 1983, ApJ, 265, 620
- Romero, G. E., Vieyro, F. L. and Villa, G. S. 2010b, A&A 519, A109
- Singh, C. B., de Gouveia Dal Pino, E. M., & Kadowaki, L. H. S. 2015, ApJL, 799, L20 (SGK15)
- Sironi, L., & Spitkovsky, A. 2014, ApJ, 783, 21
- Somov, B. V. 2012, *Plasma Astrophysics, Part I: Fundamentals and Practice*, Astrophysics and Space Science Library, 391
- Spruit, H. C. 1988, A&A, 194, 319
- Spurio, M. 2015, Publications of the American Astronomical Society, page 322
- Stecker, F. W. 1968, Phys. Rev. Lett., 21, 1016
- Stecker, F. W. 1970, Ap&SS, 6, 377
- Stecker, F. W. 1971, NASA Special Publication, 249, 499
- Stecker, F. W. 1979, ApJ, 228, 919
- Stecker, F. W., Done, C., Salamon, M. H., & Sommers, P. 1991, PhRvL, 66, 2697
- Tavecchio F., Ghisellini G. & Guetta D., 2014, ApJ, LL18
- Tavecchio, F., & Ghisellini, G. 2014, arXiv:1411.2783
- Vila G. S. and Aharonian F. 2009, Asociaon Argentina de Astronomia- Book Series, AAABS, Vol. 1, 2009
- Vincent, S., 2014, arXiv:1411.1957
- Waxman, E. & Bahcall, J. N. 1997, Physical Review Letters, 78, 2292
- Yamada, M., Jongsoo, Y., Jonathan J. A., Hantao, J., Russell M. K. & Clayton E. M. 2014, Nature Communications 5, 4774
- Yuan, Z., & Wang, J. 2012, ApJ, 744, 84
- Zenitani, S. and Hoshino, M. 2001, ApJ, 562L, 63Z

This paper has been typeset from a \TeX / \LaTeX file prepared by the author.